Radiation Physics and Chemistry (xxxx) xxxx–xxxx

Contents lists available at ScienceDirect

Radiation Physics and Chemistry

journal homepage: www.elsevier.com/locate/radphyschem

Characterization of detector-systems based on $CeBr_3$, $LaBr_3$, SrI_2 and CdZnTe for the use as dosemeters

P. Kessler*, B. Behnke, H. Dombrowski, S. Neumaier

Physikalisch-Technische Bundesanstalt, Bundesallee 100, 38116 Braunschweig, Germany

ARTICLE INFO

Keywords:
Environmental monitoring
Scintillation detectors
Monte-Carlo simulations

ABSTRACT

For the upgrade of existing dosimetric early warning networks in Europe spectrometric detectors based on $CeBr_3$, $LaBr_3$, SrI_2, and CdZnTe are investigated as possible substitutes for the current detector generation which is mainly based on gas filled detectors. The additional information on the nuclide vector which can be derived from the spectra of γ-radiation is highly useful for an appropriate response in case of a nuclear or radiological accident.

The measured γ-spectra will be converted into ambient dose equivalent $H^*(10)$ using a method where the spectrum is subdivided into multiple energy bands. For each band the conversion coefficients from count rate to dose rate is determined. The derivation of these conversion coefficients is explained in this work. Both experimental and simulative approaches are investigated using quasi-mono-energetic γ-sources and synthetic spectra from Monte-Carlo simulations to determine the conversion coefficients for each detector type. Finally, precision of the obtained characterization is checked by irradiation of the detectors in different well-known photon fields with traceable dose rates.

1. The existing early warning networks and the MetroERM project

After the Chernobyl accident in 1986, all European countries installed early warning networks, each of which comprises a number of dosimetric monitoring stations distributed over the countries. Today, more than 5000 stations exist in Europe. Most of them are based on gas filled detectors such as Geiger-Muller counters or proportional counters. While these stations deliver information about dose rates, other instruments are needed for information about the nuclide vector. The latter can be achieved, e.g., by using scintillation detectors or conventional HPGe detectors which need cooling with liquid nitrogen. Currently very few countries operate such stations. Finland, for example uses $LaBr_3$ based detectors (Toivonen et al., 2008).

One of the key tasks of the MetroERM project (Neumaier et al., 2016) is to characterize spectro-dosemeters to see if they can replace the existing dosimetric systems. These relatively new scintillation detectors have a far better energy resolution (3–4%) compared with NaI(Tl) (best: 6%). In case of a radiological emergency they are suitable for the identification of nuclides causing local contaminations and, hence, facilitate appropriate countermeasures. Once the project is complete, a best practice guide will be developed and guidance on how best to implement these systems will be given. The existing EURDEP database (de Vries et al., 2005) where the dose rate information of the stations is stored is already able to include information about the nuclide vector.

2. Calculation of dose rate values from γ-spectra

This work concentrates on the conversion from spectral information of γ-radiation into dose rates. Several methods are described in detail in reference (Dombrowski, 2014). The method used for this work was chosen because of its simplicity. The spectrum is subdivided into multiple energy bands and for each band the conversion coefficient w_i from counts to ambient dose equivalent $H^*(10)$ (Petoussi-Henss et al., 2010) is determined (Fig. 1). It can be shown (Dombrowski, 2014) that the pulse height vector $\vec{n}$ of the spectrum can be converted by a vector $\vec{v}_H$ to $H^*(10)$ (scalar product, see Eqn. (1)). $\vec{v}_H$ consists of the elements $w_i \cdot E_i$, where E_i is the mean energy of the i^{th} band and w_i the corresponding conversion coefficient. When all w_i are determined the $H^*(10)$ value for a spectrum $\vec{n}$ can be calculated as follows:

$$H^*(10) = \vec{n} \cdot \vec{v}_H = \sum_i n_i \cdot w_i \cdot E_i \tag{1}$$

For each detector system a full set of w_i is derived using spectra from quasi-mono-energetic γ-sources or synthetic spectra from Monte-Carlo (MC) simulations. The first band (i = 1) at the lowest energy can

* Corresponding author.

http://dx.doi.org/10.1016/j.radphyschem.2016.12.015
Received 30 September 2016; Accepted 24 December 2016

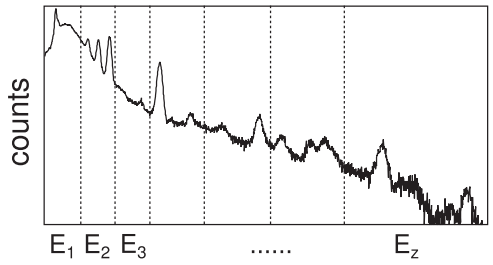

Fig. 1. The spectrum is divided into z bands with the mean energy E. For each band the corresponding conversion coefficient w_i from counts to $H^*(10)$ is measured with quasi-mono-energetic radioactive sources.

be calculated with the $H^*(10)$ value of a photon field of a radioactive source which only has emission lines in this energy band (i=1):

$$w_i = \frac{H^*(10)_{\text{band}}}{n_i \cdot E_i} \tag{2}$$

When the subsequent w_i of higher energy bands are calculated, the previously measured w_i have to be taken into account, because some of the incident photons deposit only part of their energy in the detectors due to various scattering processes (e.g. Compton-effect or escape photons following pair production). Therefore the dose $H^*(10)_{\text{det}}$ from the lower energy part of the spectrum where the w_i are already determined has to be calculated (see Eq. (1)) and subtracted from the total dose the detector was irradiated with ($H^*(10)_{\text{total}}$). The new w_i is calculated with the remaining dose $H^*(10)_{\text{band}} = H^*(10)_{\text{total}} - H^*(10)_{\text{det}}$ attributed to its band.

3. Experimental procedure and results

In the following the sources used and a full set of w_i is listed for each of the detector systems. These detectors were assembled from commercially available components which were installed into an aluminum housing.

The scintillation crystals ($CeBr_3$, $LaBr_3$, SrI_2) are of cylindrical shape with a diameter and height of 2.54 cm (1 in.). The CdZnTe semiconductor detector has a cubical shape with side lengths of 1 cm. Photomultipliers (PM) of the type *Hamamatsu R6231* were used. The signal of the $CeBr_3$ and $LaBr_3$ crystals was read out by an *Ortec digiBase-E*, that of the SrI_2 crystal by a *Base 527* manufactured by *GBS Elektronik*. The CdZnTe-detector system *GR1-Gamma Ray Spectrometer* was obtained from *Kromek*.

3.1. Measurements of the conversion coefficients w_i

The corresponding w_i for each energy band was determined using quasi-mono-energetic sources (described in Section 2). In a previous study the inherent background, which has to be subtracted from the obtained spectra was measured (Kessler et al., 2016).

The energy range of each band is determined by the peak energy of the source which should be in the center of the band. In Table 1 the sources used, their main emission lines and the corresponding energy ranges of the bands are summarized. In the energy range from 122 keV to 440 keV no source was available. Instead, the N-300 X-ray quality as described in the standard ISO 4037-1:1996 (International Organization for Standardization,1996) was used which is available in PTB's 400 kV X-ray facility.

3.2. Angular dependence of the response

For the method described above (Eq. (1)) the angular dependence of the detector response to γ-radiation has to be taken into account. Therefore, the detectors were irradiated from different angles (from 0° to 130°, the definition of the angles can be found in Fig. 2) with two different energies: 60 keV (^{241}Am) and 662 keV (^{137}Cs).

Table 1
Radioactive sources used in this work, the energies of their main emission lines and the corresponding ranges of each energy band. One band was covered using the N-300 X-radiation quality available at the 400 kV X-ray facility at PTB (in this case the mean energy stated in the second column is that of the X-ray spectrum). Emission lines not used for the determination of the conversion coefficients are written in italics.

Source	Main energies above 40 keV in keV	Band range keV
^{241}Am	60	40–80
^{109}Cd	88	80–96
^{57}Co	122	96–148
N–300	247	148–346
^{192}Ir	*296*, *308*, *316*, 468, *604*	346–538
^{137}Cs	662	538–846
^{60}Co	1173, 1333	846–1654
^{88}Y	*898*, 1836	1654–2018

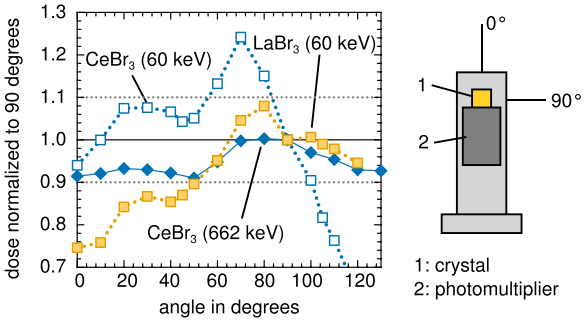

Fig. 2. Relative angular dependence of the detector response to 60 keV (^{241}Am) and 662 keV (^{137}Cs) γ-radiation and definition of the angles. Depending on the design of the system, at low energies absorption effects are highly dependent on the angle of incidence ($LaBr_3$). At high energies above 662 keV the angle of incidence is almost negligible.

The results are shown in Fig. 2 where $LaBr_3$ and the $CeBr_3$ based system are compared. At 60 keV the $CeBr_3$ based system in contrast to the $LaBr_3$ based system shows a strong angular dependence which cannot be seen at 662 keV. The main reason is a metal shielding of the PM which absorbs the low energy γ-rays. In the case of a large homogeneous surface contamination as a consequence of a radiological accident where the dominant part of the γ-radiation is detected from an angular range from 90° to 105°, the angular dependence can be neglected in good approximation, even at low energies.

3.3. Resulting conversion coefficients w_i

The final results of the experimental determination of conversion coefficients w_i are listed in Table 2. The uncertainties are estimated with a MC model that varies the counts (from statistical origin) in the

Table 2
Resulting conversion coefficients w_i for all detector systems (in 10^{-15} Sv, according to Eq. (2)). The uncertainties are estimated using a Monte-Carlo method. For comparison, the results of the Monte-Carlo simulation of the SrI_2 based system is given in the last two columns.

E_{mean} keV	$CeBr_3$ fSv/keV	$LaBr_3$ fSv/keV	SrI_2 fSv/keV	CdZnTe fSv/keV	E_{mean} keV	SrI_2 (MC) fSv/keV
60	2.49 ± 0.06	1.73 ± 0.04	3.51 ± 0.08	12.0 ± 0.3	60	2.03
88	0.95 ± 0.05	0.86 ± 0.04	0.82 ± 0.05	5.8 ± 0.4	90	1.14
122	1.16 ± 0.02	1.03 ± 0.02	1.10 ± 0.02	7.2 ± 0.2	120	1.03
247	1.35 ± 0.03	1.36 ± 0.03	1.33 ± 0.03	10.9 ± 0.3	240	1.51
442	3.3 ± 0.5	3.0 ± 0.5	3.2 ± 0.5	35 ± 5	415	3.46
662	3.5 ± 0.3	3.3 ± 0.3	3.5 ± 0.2	40 ± 5	715	3.85
1250	3.45 ± 0.07	3.43 ± 0.07	3.77 ± 0.07	43 ± 2	1165	3.85
1836	4.3 ± 0.8	4.0 ± 0.8	4.6 ± 0.8	53 ± 16	2315	4.07